

Synthesis and characterizations of Nano magnetic particles (Co-Ni Fe₂O₄) ferrite by co-precipitation and biomedical application

Marwa H. Sabbar¹, T. H. Mubarak¹, Nada S. Ahmad¹

¹Department of Physics, College of Science, University of Diyala, Diyala, Iraq

Received 16 May 2022, Revised 21 July 2022, Accepted 4 August 2022

Abstract

*Characterization of Co_{x-1}Ni_x Fe₂O₄ nanoparticles (NPs) employing X-ray diffraction and field emission scanning electron microscopy (FESEM) was accomplished simply by chemical co-precipitation, FTIR, and finally the Magnetic Resonance Spectrometer (VSM). The single-phase cubic spinel structure in X-Ray diffraction. In FESEM show micrographs of Co ferrites nanoparticles that are virtually spherical and have grain sizes of less than 20 nm. Two absorption bands are visible in the FTIR spectrum, with values ranging from 400-600 cm. These beams show that all of the samples have a ferrite spectral composition. Preparation of samples yielded M-H Curves Because of the tight turn, which means the paper samples are soft magnetic material in the VSM. Antibacterial activity of Co_{x-1}Ni_x Fe₂O₄ NPs in limiting the development of isolated pathogenic bacteria *Staphylococcus aureus* and *E. coli* was studied to compare their effects with the traditional antibiotics used before. Using Co_{x-1}Ni_x Fe₂O₄ nanoparticles, it has been found that the nanoparticles release ions into the environment, which interacts with the group (-SH) of proteins, resulting in the defection of bacteria's cell membranes and the subsequent cell death.*

Keywords: Pulsed laser deposition (PLD), Co-Ni ferrite, antibacterial of Co-Ni ferrite.

1. INTRODUCTION

The topic of nanotechnology has advanced dramatically in recent decades, particularly in the physical sciences [1]. The ability to make ferrite nanoparticles has opened up a fascinating new field of research, with revolutionary possibilities not only in electrical technology but also in biotechnology [2]. Over the last decade, the use of metallic nanoparticles (NP) has increased dramatically. including biomedical and other sectors. At this time, Substantial studies have been carried out on the subject. production of metallic nanostructures and the study of their applications on a large scale [3- 6]. For magnetic reasons, NP for iron, cobalt, and nickel is regarded as among the many forms of nanostructures created [7]. Due to its unusual features, particularly magnetic and electromagnetism, NP magnetism has sparked a lot of attention and has been employed in a variety of applications [8-12]. In general, MFe₂O₄ is a formula for magnetic materials (M: divalent metal ion, such as Mn, Mg, Zn, Ni, Co, Cu, and others) [13]. They offer a lot of potential for use because of their unique features electronics [14], catalyst [15], battery [16], antimicrobial agents, magnetic storage devices, and other medical disciplines [17], immunoassay [18], heat therapy [19] and magnetic resonance photography [20]. Cobalt ferrite is a well-known substance with a strong magnetic field. Magnetization saturation and a material with a high coercive strength. Despite its low coactivity and saturation magnetization, despite being a soft material, ferrite nickel has a high coercive strength and saturation magnetization when compared to other materials. They are great candidates for a wide range of biological, electrical, and recording applications to several of these characteristics (hard and soft magnetic). [21-24]. From the standpoint of

Note: Accepted manuscripts are articles that have been peer-reviewed and accepted for publication by the Editorial Board. These articles have not yet been copyedited and/or formatted in the journal house style

magnetic applications, nanoparticles' nature is mostly determined by their size and form. For these nanoparticles, magnetic purity and stability (such as super magnetic blocking at a given temperature, etc.) are important [25].

2. Experimental work

2.1 Materials

Ferrite powders were prepared, cobalt nitrate, iron nitrate and nickel nitrate were used as starting materials. Table (1) shows the raw materials and their density.

Table 1 Chemicals Used.

Compounds	Chemical formula	Mol. Mass (g. mol-1)
Iron nitrate	$\text{Fe}(\text{NO}_3)_{2.9}\text{H}_2\text{O}$	403.8
Cobalt nitrate	$\text{Co}(\text{NO}_3)_{2.6}\text{H}_2\text{O}$	291.031
Nickle nitrate	$\text{Ni}(\text{NO}_3)_{2.6}\text{H}_2\text{O}$	290.79
Sodium hydroxide	NaOH	39.9971

2.2 Sample Preparation

Ferrites nanomaterials with the formula $\text{Co}_{1-x}\text{Ni}_x\text{Fe}_2\text{O}_4$ "x = 0.0, 0.2, and 0.4" are created using "chemical co-precipitation". To make ferrite samples, molar quantities that are stoichiometric All three nickel and cobalt (II) nitrates [$\text{Ni}(\text{NO}_3)_{2.6}\text{H}_2\text{O}$], $\text{Co}(\text{NO}_3)_{2.6}\text{H}_2\text{O}$, and ferric nitrate $\text{Fe}(\text{NO}_3)_3 \cdot 9\text{H}_2\text{O}$] Merck accounts for 98.5 percent of the total were used. With steady magnetic stirring, ferric nitrate, nickel nitrate, and cobalt nitrate dissolve in de-ionized water. As a precipitation agent, a (1.5M) NaOH solution is utilized. Once the PH of the combination hits 12, we heat it at 80 ° C for 30 minutes to precipitate the components. The precipitates are then rinsed with deionized water many times until the pH level of the solution returns to normal (pH =7-8). At 125°C, the product precipitates are dried. to remove the water, then ground into powder and asserted in an electric furnace at 300 °C for 3 hours to get the ferrite phase of spinel

3. Results and Discussions

3.1 XRD diffraction

The crystal structure and purity of the material can be determined using XRD. Figure 1 illustrates a specimens' XRD spectra. $\text{Ni}_{1-x}\text{Co}_x\text{Fe}_2\text{O}_4$, "x = 0.0, , 0.2, , and 0.4" Xray diffraction patterns at 300 °C for 3 h reveal, a cubic spinel-structured pure phase (JCPDS card number 40-1191). There are numerous peaks in the poly-oriented polygonal structure that indicate unique crystallite planes in the single-phase cubic spinel structure. $\text{Ni}_{1-x}\text{Co}_x\text{Fe}_2\text{O}_4$, "220, 311, 222, 400, 422, 511, and 440".

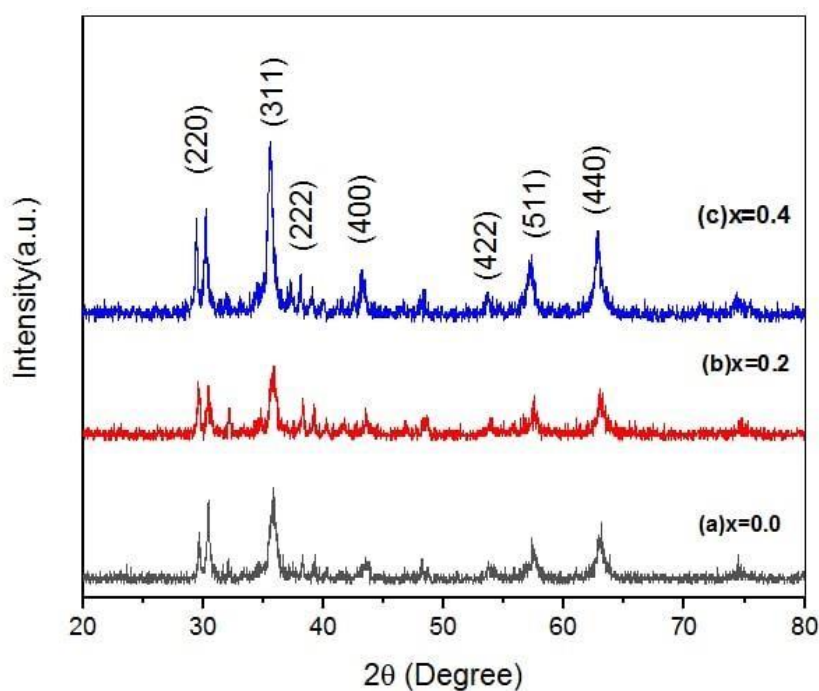


Figure 1. XRD Patterns for $\text{Co}_{1-x}\text{Ni}_x\text{Fe}_2\text{O}_4$.

Table 2 XRD parameters of synthesized $\text{Ni}_x\text{Co}_{1-x}\text{Fe}_2\text{O}_4$

Material	Ratio	2θ (deg) Practical	2θ (deg) Standard	FWHM size (nm)	Crystalline Practical	d_{hkl} (°A) (deg)	d_{hkl} (°A) Standard	(hkl)
CoFe_2O_4	0	35.69	35.63	0.6985	10.82	2.513681	2.5176	(113)
$\text{Ni}_{0.2}\text{Co}_{0.8}\text{Fe}_2\text{O}_4$	0.2	35.64	35.63	0.5675	13.32	2.517093	2.5176	(113)
$\text{Ni}_{0.4}\text{Co}_{0.6}\text{Fe}_2\text{O}_4$	0.4	35.69	35.63	0.6382	14.31	2.513681	2.5176	(113)

3.2 FTIR spectroscopy

They're called ferrites because they're made up of atoms that are "connected to all their nearest neighbors by the equivalent strength of ionic, covalent, or van der Waals interactions." From a wave number range (350 to 4000 cm^{-1}), the FTIR spectra of $\text{Ni}_x\text{Co}_x\text{Fe}_2\text{O}_4$ have been obtained are shown in Fig. 2. The metal ions in ferrites occupy two distinct sub-lattices in reference to the geometrical arrangement of oxygen's nearest neighbors, identified as tetrahedral "A-site" and octahedral "B-site." Wave numbers are greater in ν_1 , that can be seen in the range of 580–600 cm^{-1} , this is the vibration of the metal at the tetrahedral site "Mtetra \leftrightarrow O". There was a lower wave number one than there was,"usually observed around 375–450 cm^{-1} " is attributed to octahedral

stretching "Moctao" [18, 19], In addition to vibrations in the NO₃ ion, the carboxyl group COO⁻, and the stretching of the C-H bands and hydrogen bound O-H groups, It is possible to see "1100–1300" cm⁻¹, "1400–1700" cm⁻¹, 2850–3000" cm⁻¹, and 3400cm⁻¹ weaker absorbance bands at the margins. respectively. [20, 21]. The octahedral and tetrahedral complexes' change in Fe³⁺-O²⁻ ion distance is responsible for the notable shift in band locations. Interestingly, as the Co substitution content increases, the characteristic band 1 shifts towards lower and higher frequency regions. table (3) shows the limits of the absorption bands of the compound.

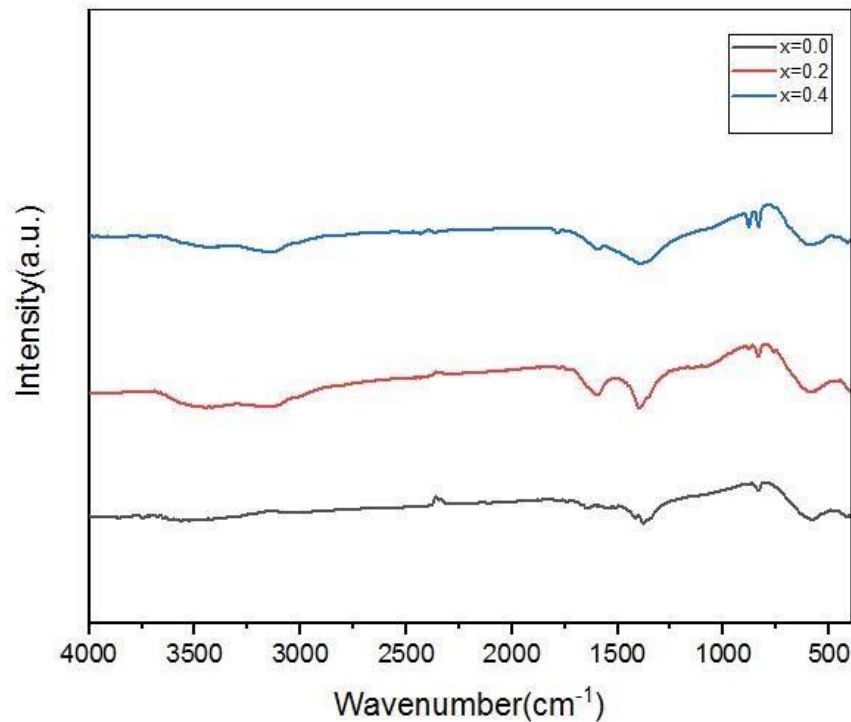


Figure 2. show the FTIR spectra of Ni_{1-x}Co_xFe₂O₄.

Table 3 IR absorption bands and force constants of the Co_{1-x}Ni_xFe₂O₄ samples.

X	U _T cm ⁻¹	U _B cm ⁻¹
0.0	596.602	378.009
0.2	595.269	375.341
0.4	591.267	375.341

3.3 Magnetic measurements

A magnetometer (VSM) is being used to investigate magnetic properties at room temperature of the produced samples. "Fig. 3" shows the M-H curves of the samples that have been prepared The loop is narrow, which means the paper samples are soft magnetic material. In the applied field, AS nano samples reach saturation magnetization, As shown

Note: Accepted manuscripts are articles that have been peer-reviewed and accepted for publication by the Editorial Board. These articles have not yet been copyedited and/or formatted in the journal house style

in the insert of figures, coercivity (H_C) and saturation magnetization (M_s) values were extracted directly from these curves. All prepared samples of Co-Ni ferrite ($x = 0, 0.2, \text{ and } 0.4$) "at room temperature exhibit ferrimagnetic coupling". At room temperature, Ni concentration lowers both saturation magnetization and coercivity. The process of superexchange contact causes magnetic order in cubic spinels. between the metal ions in their A-sites and B-sites, which makes them more magnetic than other spinels.

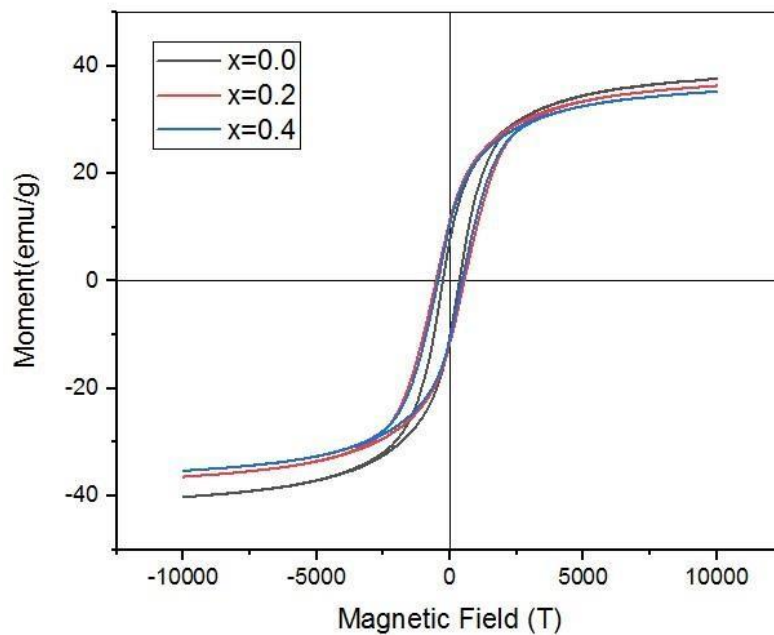


Figure 3. Room temperature M-H hysteresis loop for $CO_{1-x}Ni_xFe_2O_4$ system.

Table 4 shows the values of saturation magnetization, residual magnetization and force field values of nickel cobalt ferrite.

Molar ratio	M_s (emu/g)	M_r (emu/g)	H_c (kOe)
0.0	35.551	11.475	0.002
0.2	34.660	11.355	0.025
0.4	24.601	9.205	0.016

3.4 FESEM analysis

It shows FESEM micrographs of Co ferrites nanoparticles that are virtually spherical and have grain sizes of less than 20 nm. Furthermore, despite the fact that These tiny crystallites are equally distributed across the area, showing the development of fine granularity due to magnetic nanoparticle interactions, Agglomeration can occasionally reveal a visible boundary between nearby crystallites.

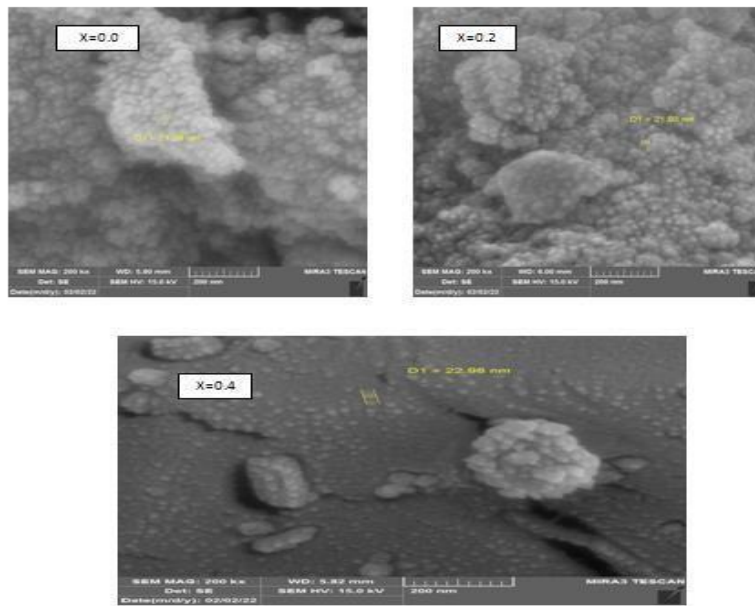


Figure 4. FE- SEM image of $\text{Co}_{1-x}\text{Ni}_x\text{Fe}_2\text{O}_4$

3.5 Antibacterial activity of $\text{Co}_{x-1}\text{Ni}_x\text{Fe}_2\text{O}_4$ ferrite

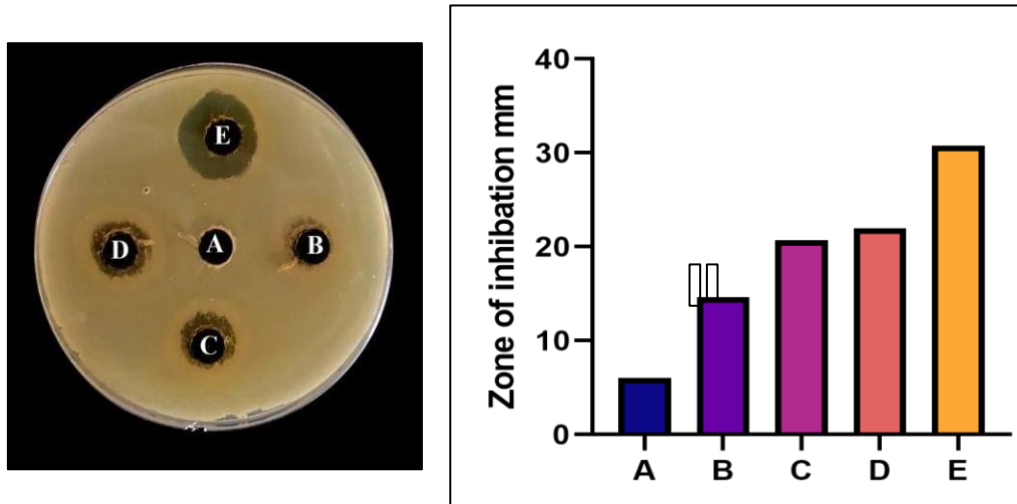


Figure 1: Antibacterial activity of (sample 4) against *E.Coli*. A control. B, 25%. C, 50%. D, 75%. E, 100%.

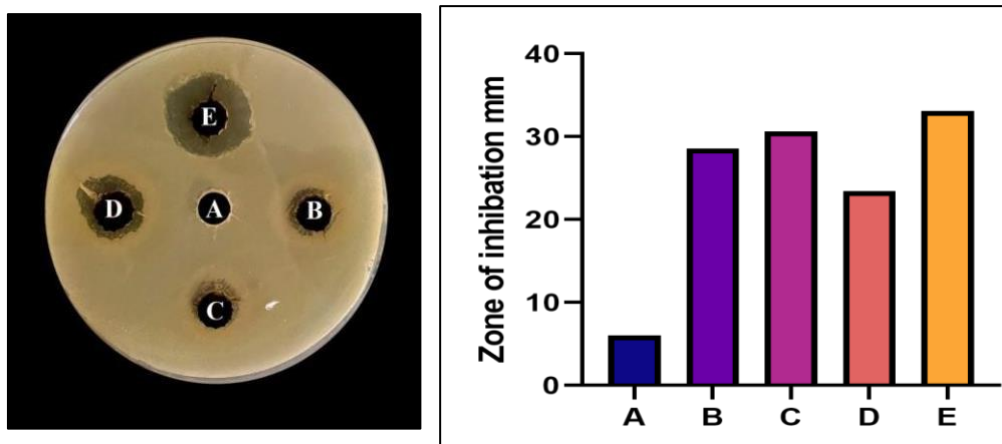


Figure 2: Antibacterial activity of (sample 2) against *E.Coli*. A control. B, 25%. C, 50%. D75%. E, 100%.

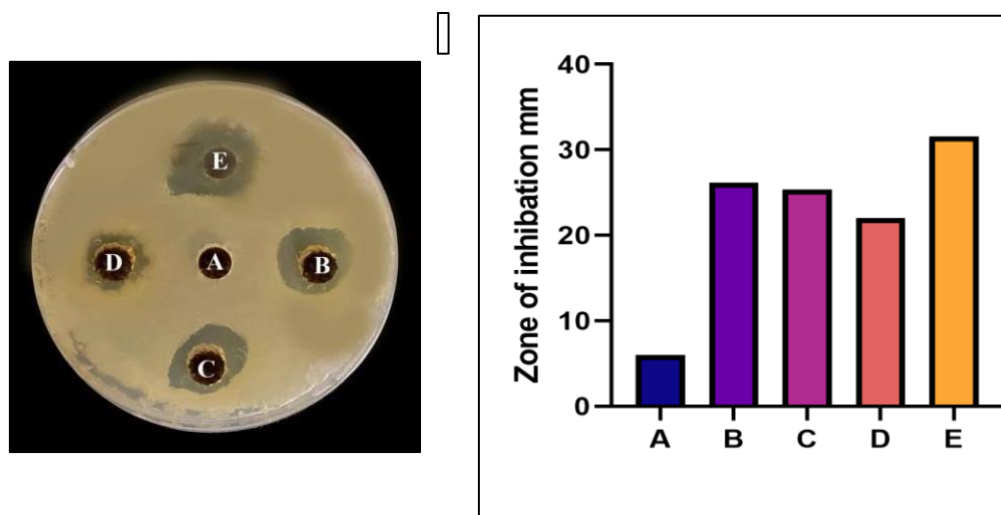


Figure 3: Antibacterial activity of (sample 3) against *E.Coli*. A control. B, 25%. C, 50%. D75%. E, 100%.

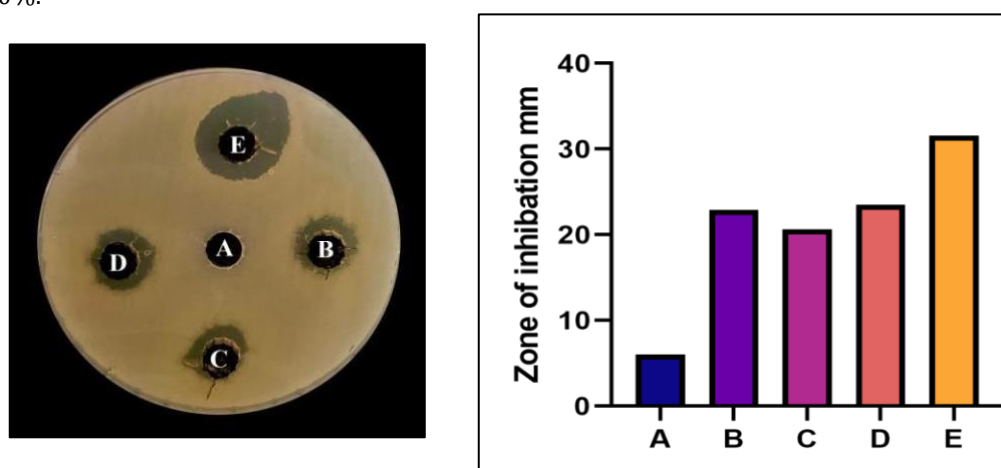


Figure 4: Antibacterial activity of (sample1) against *S. aureus*. A control. B, 25%. C, 50%. D75%.

E,

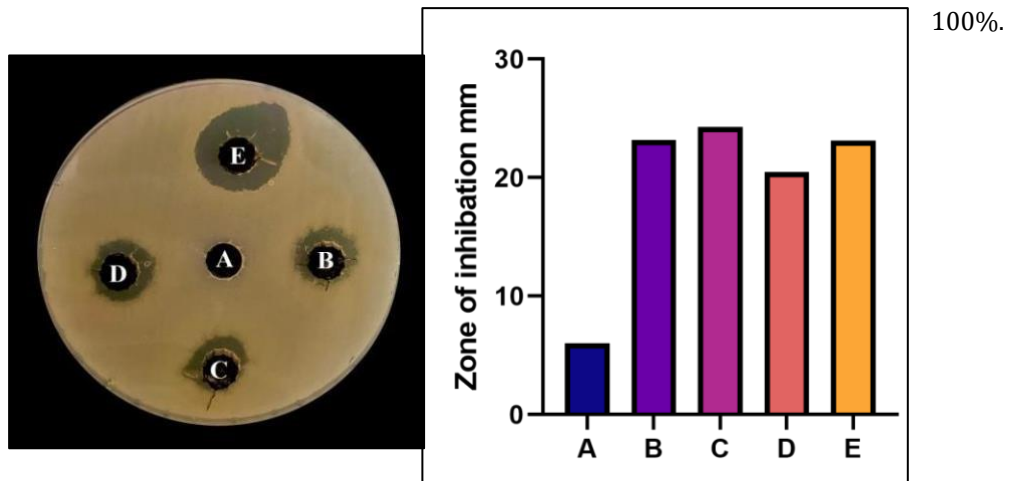


Figure 5: Antibacterial activity of (sample 2) against *S. aureus*. A control. B,25%.C,50%.D75%.E, 100%.

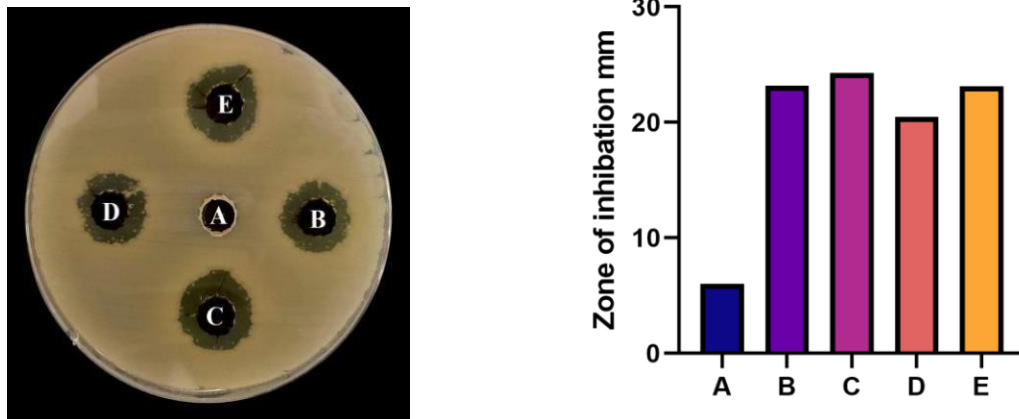


Figure 1: Antibacterial activity of (sample 3) against *S. aureus*. A control. B,25%.C,50%.D75%.E, 100%.

Table 1 The results of the inhibition zone for Co-Ni-Fe₂O₄ ferrite by methods, co-precipitation, Antibacterial activity of NPs against gram-negative (*E. coli*)

SAMPLES	A	B	C	D	E
1	6	14.635	20.686	21.965	30.798
2	6	28.565	30.639	23.457	33.131

3	6	26.145	25.375	22.053	31.571
---	---	--------	--------	--------	--------

Table 2 Results of the inhibition zone for Co-Ni -Fe₂O₄ ferrite by co- n techniques Antibacterial activity o

SAMPLES	A	B	C	D	E
1	6	22.917	20.634	23.512	31.553
2	6	23.18	24.274	20.453	23.137
3	6	21.145	24.653	24.885	23.562

1. CONCLUSION

At 300 °C for 3 hours, chemical co-precipitation was used to make cobalt replaced nickel spinel nanoparticles. The cubic spinel phase is seen in the ferrite samples' XRD patterns. As established by X-ray diffraction, the size of a single cubic spinel structure ranging from 16 to 19 nm is the typical crystalline size of ferrite nanoparticles. The nanocrystal lines in the produced products are confirmed by FESEM pictures. Infrared spectroscopy of the ferrite powders reveals two distinct bands in the 500-600 cm⁻¹ and 385-450 cm⁻¹ wavelength range, It is possible that the tetrahedral and octahedral complexes are responsible. High-quality ferrite nanopowder can be made using a simple and low-cost process called co-precipitation.

REFERENCES

- [1] Sagadevan, S., Chowdhury, Z. Z., & Rafique, R. F." Preparation and characterization of nickel ferrite nanoparticles via co-precipitation method". *Materials Research*, 21 (2018).
- [2] Valenzuela, R. "Novel applications of ferrites". *Physics Research International*, 2012.
- [3] Khorasani-Motlagh M., Noroozifar M., Jahani S. "Preparation and characterization of nano-sized magnetic particles LaCoO₃ by ultrasonic-assisted coprecipitation method. *Synth React Inorg M.*" 45(10):1591–1595;2015.
- [4] Singh, P., Yu-Jin K., Dabing Z., and Deok-Ch. Y.. "Biological synthesis of nanoparticles from plants and microorganisms." *Trends in biotechnology* 34, no. 7 (2016): 588-599.
- [5] Singh, H., Du, J., Singh, P., & Yi, T. H. "Extracellular synthesis of silver nanoparticles by *Pseudomonas* sp. THG-LS1. 4 and their antimicrobial application". *Journal of pharmaceutical analysis*, 8(4), 258-264, (2018).
- [6] Alijani, H. Q., Pourseyedi, S., Mahani, M. T., & Khatami, M. Green synthesis of zinc sulfide (ZnS) nanoparticles using *Stevia rebaudiana* Bertoni and evaluation of its cytotoxic properties. *Journal of Molecular Structure*, 1175, 214-218; (2019).

- [7] Rathi A., Meka V. M., Jayaraman TV. "Synthesis of nanocrystalline equiatomic nickelcobalt-iron alloy powders by mechanical alloying and their structural and magnetic characterization. *J Magn Mater.*;469:467–482;2019.
- [8] Boruah P. K., Borthakur P., Das MR. Magnetic metal/metal oxide nanoparticles and nanocomposite materials for water purification. In: *Nanoscale materials in water purification*. Netherlands: Elsevier. p. 473–503; 2019.
- [9] Khatami, M., Iravani, S., Varma, R. S., Mosazade, F., Darroudi, M., & Borhani, F. Cockroach wings-promoted safe and greener synthesis of silver nanoparticles and their insecticidal activity. *Bioprocess and biosystems engineering*, 42(12), 2007-2014 ;(2019).
- [10] Gholami L, Kazemi Oskuee R, Tafaghodi M, et al." Green facile synthesis of low-toxic superparamagnetic iron oxide nanoparticles (SPIONs) and their cytotoxicity effects toward Neuro2A and HUVEC cell lines." *Ceram Int.*44(8):9263; 2018
- [11] Seddighi N. S., Salari S., Izadi A. R." Evaluation of antifungal effect of iron-oxide nanoparticles against different *Candida* species." *IET Nanobiotechnol.*11(7):883. 2017
- [12] Mirzaei, H., Nasiri, A. A., Mohamadee, R., Yaghoobi, H., Khatami, M., Azizi, O., ... & Azizi, H. Direct growth of ternary copper nickel cobalt oxide nanowires as binder-free electrode on carbon cloth for nonenzymatic glucose sensing. *Microchemical Journal*, 142, 343-351; 2018.
- [13] Chaibakhsh N, Moradi-Shoeili Z." Enzyme mimetic activities of spinel substituted nanoferrites (MFe₂O₄): a review of synthesis, mechanism and potential applications. *Mat Sci Eng C*. 99: 1424–1447;2019.
- [14] Demir L., Peris,anoglu U., S. ahin M. Investigating XRF parameters and valance electronic structure of the Co, Ni, and Cu spinel ferrites. *Ceram Int*".45(6):7748–7753;2019.
- [15] Anwar A, Yousuf MA, Tahir B, et al. New Er³⁺-substituted NiFe₂O₄ nanoparticles and their nano-heterostructures with grapheme for visible light-driven photo-catalysis and other potential applications. *CNANO*.;15(3):267–278; 2019.
- [16] Cherian C. T., Sundaramurthy J, Reddy M, et al. Morphologically robust NiFe₂O₄ nanofibers as high capacity Li-ion battery anode material. *ACS Appl Mater Interfaces* .5(20):9957–9963;2013.
- [17] Jose, J., Thomas, S., Kalarikkal, N., & Oluwafemi, O. S. Antimicrobial properties of MFe₂O₄ (M= Mn, Mg)/reduced graphene oxide composites synthesized via solvothermal method. *Materials Science and Engineering: C*, 95, 43-48; (2019).
- [18] Karmakar, S., Routray, K. L., Panda, B., Sahoo, B., & Behera, D. Construction of core@ shell nanostructured NiFe₂O₄@ TiO₂ ferrite NAND logic gate using fluorescence quenching mechanism for TiO₂ sensing. *Journal of Alloys and Compounds*, 765, 527-537; (2018).
- [19] Sangeetha K, Ashok M, Girija E. Development of multifunctional cobalt ferrite/hydroxyapatite nanocomposites by microwave assisted wet precipitation method: a promising platform for synergistic chemo-hyperthermia therapy. *Ceram Int.*45(10): 12860; 2019.
- [20] Hankiewicz, J. H., Stoll, J. A., Stroud, J., Davidson, J., Livesey, K. L., Tvrdy, K., ... & Celinski, Z. JNano-sized ferrite particles for magnetic resonance imaging thermometry. *Journal of Magnetism and Magnetic Materials*, 469, 550-557;(2019).

- [21] Maaz, K., Karim, S., Mashiatullah, A., Liu, J., Hou, M. D., Sun, Y. M., Chen, Y. F.. Structural analysis of nickel doped cobalt ferrite nanoparticles prepared by coprecipitation route. *Physica B: Condensed Matter*, 404(21), 3947-3951;(2009).
- [22] S.D. Bader, Rev. Modern Phys. 78 1;(2006).
- [23] C.A. Ross, Ann. Rev. Mater. Res. 31 203; (2001).
- [24] R.W. Wood, J. Miles, T. Olson, IEEE Trans. Magn. 38 (4) (2002) 1711
- [25] K. Maaz a,, S. Karim a , A. Mashiatullah et al." " Structural analysis of nickel doped cobalt ferrite nanoparticles prepared by coprecipitation route." *Physica B* 404 3947–3951; (2009)

